Numerical investigations of shear strain localization in an elasto-plastic Cosserat material

Investigations numériques sur les déformations en cisaillement dans un matériau élastoplastique de type Cosserat

Ebrahimian B.
School of Civil Engineering, Faculty of Engineering, University of Tehran, Tehran, Iran

Noorzad A.
Faculty of Water and Environmental Engineering, Power and Water University of Technology, Tehran, Iran

ABSTRACT: The phenomenon of strain localization in narrow zones, called shear bands, is mainly related to the micro-structure of granular materials. This phenomenon cannot be modeled properly within the framework of classical continuum especially in the post-bifurcation regime due to the lack of characteristic length of the micro-structure. For finite element calculations, Cosserat (micro-polar) continuum is an effective regularization technique to remove the numerical difficulties when shear localization occurs. The paper presents numerical investigations of shear strain localization in plane shearing of an infinite granular layer as well as biaxial compression of a specimen using micro-polar (Cosserat) continuum approach. It is shown that the micro-polar effects i.e., Cosserat rotations, micro-curvatures and couple stresses are significant in the emerged shear bands. Shear banding pattern is significantly affected by the prescribed micro-polar boundary conditions of entire system as well as geometry of specimen. It is confirmed that the proposed elasto-plastic Cosserat model is capable to predict the evolution of micro-polar effects within the shear band.

RÉSUMÉ : Le phénomène de localisation des contraintes dans des zones étroites, appelées bandes de contraintes, est principalement présent dans des microstructures de matériaux granulaires. Ce phénomène ne peut pas être modélisé correctement au moyen de continuum classique, en particulier pour un régime de postbifurcation, à cause du manque de critères de longueur des microstructures. Pour des calculs par éléments finis, un continuum Cosserat (micropolaire) est un moyen technique qui permet de supprimer les difficultés numériques lorsque des cisaillements apparaissent. Cet article présente les investigations numériques de déformations en cisaillement en plan pour une couche granulaire infinie ainsi que la compression biaxiale d'un spécimen en ayant recours à un continuum micropolaire (Cosserat). Il est montré que les effets micropolaires, comme les rotations Cosserat, les micros-courbures et les couples de contraintes sont significatifs dans les bandes de cisaillement apparentes. La structure de bandes de cisaillement est affectée de manière significative par les conditions micropolaires aux limites du système complet ainsi que par la géométrie du spécimen. Il est confirmé que le modèle élastoplastique Cosserat proposé est en mesure de prévoir l'évolution d'effets micropolaires dans la bande de cisaillement.

KEYWORDS: strain localization; micro-polar (Cosserat) continuum; characteristic length; granular materials; micro-polar effects.

1 INTRODUCTION

The evolution of shear bands in granluar bodies is strongly related to the micro-properties of material (Hall et al. 2010). Shear band thickness is influenced by the soil grain size which cannot be modeled properly with classical continuum models due to the lack of a material characteristic length. As a consequence, the shear band thickness is characterized by the element size in finite element simulations, and the predicted load-displacement curves are unreliable in the post-bifurcation regime (de Borst 1991). In order to overcome this shortcoming of classical continuum models and deal with such a complex phenomenon within the framework of continuum mechanics, micro-polar or the so-called Cosserat continuum models may be used, which offer the possibility to include the mean grain diameter as characteristic length (Mühlhaus 1986). The presence of characteristic length allows taking into account the microscopic inhomogeneities triggering shear localization (e.g. grain size, size and spacing of micro-defects) observed experimentally in granular materials. In this paper, an elasto-plastic Cosserat continuum model is proposed which takes into account micro-rotations (Cosserat rotations), micro-curvatures, non-symmetric shear stresses, and couple stresses. The mean grain diameter as characteristic length is also incorporated into the model formulations. For plane strain condition, implementation of the model in a finite element program is outlined. Due to the presence of a characteristic length of the micro-structure, the considered boundary value problems are mathematically well-posed and the shear band thickness predicted form finite element calculations is mesh independent, provided the element size is small enough. The performance of the present model is demonstrated by the numerical simulations of large monotonic plane shearing and biaxial comression leading to fully developed plastic flow. The focus of the investigations is on studying the evolution of micro-polar effects within the granular body. The influence of additional non-standard Cosserat boundary conditions on the pattern of shear banding is also considered. In particular, it is investigated how the rotation resistance of soil grains in contact with boundaries influences the location and evolution of shear localization.

2 THE ELASTO-PLASTIC COSSERAT MODEL

According to Vardoulakis and Sulem (1995), the objective or Cosserat strain rate tensor can be defined as

$$ {}^{n+1}_{n}\dot{\gamma}_{ij} = {}^{n+1}_{n}\dot{E}_{ij} + \left({}^{n}\dot{\Omega}_{ij} - {}^{n}\dot{\Omega}^{c}_{ij} \right) \tag{1} $$

where, $\dot{E}_{ij}$ = classical strain rate tensor; Ω_{ij} = classical spin tensor; Ω^{c}_{ij} = Cosserat spin tensor which is given by

$$ \Omega^{c}_{ij} = -e_{ijk}\omega^{c}_{k} \tag{2} $$

where, e_{ijk} = Ricci permutation tensor; and ω^{c}_{k} = Cosserat rotation. The micro-curvature vector of deformation or the gradient of soil grain rotation can be given by

$$ {}^{n}\kappa_{ij} = {}^{n}\omega^{c}_{j,i} \tag{3}$$

In this paper, the single hardening elasto-plastic Lade's model (Kim and Lade 1988, Lade and Kim 1988), enhanced with Cosserat rotations and couple stresses, (Ebrahimian et al. 2012), is used. The model has a non-linear elasticity function and assumes non-associative flow rule and high non-linear plastic work-based hardening function. The enhancement is carried out through the second stress and deviatoric stress invariants in order to incorporate the effects of characteristic length of micro-structure and couple stresses:

$$ J'_2 = \left\{ \left[(\sigma_{11}-\sigma_{22})^2 + (\sigma_{33}-\sigma_{22})^2 + (\sigma_{11}-\sigma_{33})^2 \right] + \left(\frac{\sigma_{12}+\sigma_{21}}{2} \right)^2 \right\} + \frac{\left(m_1^2+m_2^2\right)}{l^2} \tag{4}$$

$$ I_{II} = \frac{1}{2}\left(\sigma_{12}\sigma_{21} - \sigma_{11}\sigma_{22} - \sigma_{11}\sigma_{33} - \sigma_{22}\sigma_{33}\right) - \frac{m_1 m_2}{l^2} \tag{5}$$

where, σ_{ij} = stresses; m_i = couple stresses; and l = material characteristic length. In 2D Cosserat continuum, the stress tensor is expressed in the following vector form:

$$ \{\sigma\} = \left\{ \sigma_{11} \quad \sigma_{22} \quad \sigma_{33} \quad \sigma_{12} \quad \sigma_{21} \quad m_1/l \quad m_2/l \right\}^T \tag{6}$$

It is worth mentioning here that the stress vector is a non-symmetric vector due to the effect of couple stresses. Similarly, the objective strain vector, including strain and micro-curvature of rotations, is non-symmetric and given by

$$ \{\gamma\} = \{ \gamma_{11} \quad \gamma_{22} \quad \gamma_{33} \quad \gamma_{12} \quad \gamma_{21} \quad l\kappa_1 \quad l\kappa_2 \}^T \tag{7}$$

In finite element implementation, each node in the plane strain Cosserat continuum will have the following degrees of freedom:

$$ \{U\} = \left\{ u_1 \quad u_2 \quad \omega^c_3 \right\}^T \tag{8}$$

The constitutive relations used in the current work are homogenous in time (time-independent behavior); however, dimensionless time representation is used to avoid using the differential representation; hence, the following constitutive laws can be used:

$$ \{\dot{\sigma}\} = [D]\{\dot{\gamma}\} \tag{9}$$

where, [D] = elasto-plastic stiffness matrix in terms of both stresses and couple stresses. The present micro-polar Lade's single hardening model is implemented in a finite element program in order to investigate the phenomenon of shear localization in granular soil.

3 FINITE ELEMENT FORMULATIONS

Incorporating the Cosserat couple stresses and rotations, the virtual work equation in an updated Lagrangian reference is written as

$$ \int_{{}^{n}V} \left({}^{n+1}S_{ij}\delta\left({}^{n+1}_{n}\dot{\gamma}_{ij}\right) + {}^{n+1}m_i\delta {}^{n+1}_{n}\dot{\kappa}_i \right) dV = {}^{n+1}R \tag{10}$$

where, S_{ij} = the second Piola-Kirchhoff stress; and R = external virtual work. For finite element implementation, a quadrilateral isoparametric 4-noded element with nodal displacement and rotational degrees of freedom is formulated for plane strain condition. Geometric non-linearity is considered for finite deformation. Based on this type of element, a bi-linear shape function is used. All the internal state variables (such as stresses, plastic work, void ratio, etc.) are updated using the explicit forward Euler integration scheme. The Newton-Raphson method is employed to fulfill the static equilibrium equations. For the quadrilateral 4-noded element:

$$ \frac{\partial X_i}{\partial \xi_j} = \sum_{\mathrm{k}=1}^{4} X_i^{\mathrm{k}} \frac{\partial N^{\mathrm{k}}}{\partial \xi_j} \tag{11}$$

$$ \frac{\partial u_i}{\partial \xi_j} = \sum_{\mathrm{k}=1}^{4} u_i^{\mathrm{k}} \frac{\partial N^{\mathrm{k}}}{\partial \xi_j} \tag{12}$$

where, ξ_i = material point position at time (t) in the local co-ordinate system; X_i = material point position at time (t-Δt) in the global co-ordinate system; N = standard bi-linear shape function for computing strains, positions and etc. at nodal points. In the global system, for the body with volume (V), surface (S), total number of elements (NE) and total number of nodes (NN):

$$ \sum_{\mathrm{K}}\sum_{\mathrm{k}} \left(\int_{{}^{n+1}S} (N^T M)\, d\,{}^{n+1}S + \int_{{}^{n+1}V} I\, N^T c\, d\,{}^{n+1}V = \int_{{}^{n+1}V} B^T_{CO2} m\, d\,{}^{n+1}V \right) \tag{13}$$

$$ \sum_{\mathrm{K}}\sum_{\mathrm{k}} \left(\int_{{}^{n+1}S} (N^{T\,n+1}T)\, d\,{}^{n+1}S + \int_{{}^{n+1}V} \rho\, N^T b\, d\,{}^{n+1}V = \int_{{}^{n+1}V} B^T \sigma\, d\,{}^{n+1}V \right) \tag{14}$$

where, K (K = 1, 2, ..., NE) = element number; k (k = 1, …, 4) = node number for a given element; T = traction force; M = traction couple stress; I = first moment of inertial for the micro-medium; ρ = micro-medium density; b = body force per unit volume; c = body couple per unit volume; B_{CO2} = element matrix; and B = strain-nodal displacement matrix. In this sense, the residual load vector should be vanished to satisfy the below equilibrium equation:

$$ \sum_{\mathrm{N}} \left((\delta\omega^c)^{T\,n+1}R^m + (\delta u)^{T\,n+1}R^\sigma \right) = 0 \tag{15}$$

where, $\delta\omega^c$ is virtual Cosserat rotation; and δu is virtual displacement.

4 NUMERICAL INVESTIGATIONS OF MICRO-POLAR EFFECTS WITHIN SHEAR BANDS

For numerical investigations of the evolution of micro-polar effects in granular materials under shearing, firstly a plane granular soil layer located between very rough parallel boundaries is considered. Particularly, a section with the initial height of h_0 = 4 *cm* and the width of b = 10 *cm* is discretized by 4-noded elements. Apart from stress and displacement boundary conditions of non-polar continuum, additional non-standard micro-polar kinematical boundary conditions, i.e. couple stress and Cosserat rotation boundary conditions, must also be defined for the present model. Here, special micro-polar boundary conditions are introduced across the lateral boundaries of infinite layer due to the symmetry condition with respect to any vertical section (Ebrahimian et al. 2012). The top surface of granular layer is assumed to be fixed not to occur sliding and rotating. The vertical pressure (P_0 = 100 *kPa*) is kept constant at the top surface of layer. However, the height of layer can be changed as the result of dilation or contraction of material under shearing. Concerning the interaction between granular layer and bounding structure, it is supposed that the soil grains are captured by the very rough surface of bounding structure at the bottom. Furthermore, the vertical displacement is zero (u_2 = 0) along the bottom (x_2 = 0). A quasi-static shear deformation is initiated through constant horizontal displacement increments, prescribed at the bottom surface of granular layer. It is assumed that the granular layer is initially homogeneous and isotropic (initial void ratio = 0.6). The calibrated material constants for a dense silica sand given in (Ebrahimian et al. 2012) are used in following numerical simulations.

According to Figure 1, the Cosserat rotations have their significant values in the shear band located at the middle of layer, while outside the shear band, the values are nearly zero. These results are in accordance with the experimental observations (Hall et al. 2010). The maximum values of Cosserat rotation occurs where shear strain localization may be developed under continuous shearing. The thickness of shear band can be detected with respect to the distribution of Cosserat rotation based on its high values. This indicates that micro-polar effects in granular materials are significant when shear localization appears as also detected in experiments (Hall et al. 2010).

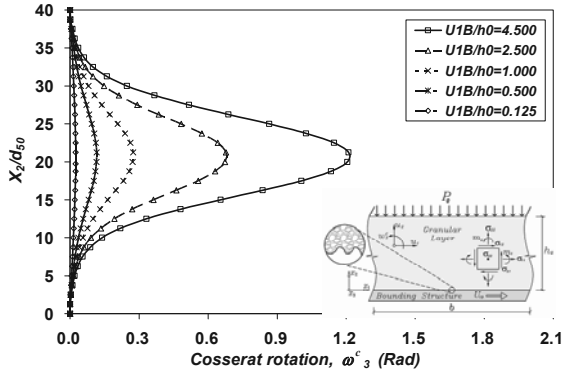

Figure 1. Distribution of Cosserat rotation across normalized height of granular layer under $P_0 = 100\ kPa$ for different U_{1B}/h_0 ($e_0 = 0.6$, $d_{50} = 1\ mm$).

The normalized micro-curvature (κ_2^*), distributed across normalized layer height, is presented in Figure 2. Based on this figure, the values of κ_2^* are high in the shear band. This result is in agreement with the numerical calculations which use discrete element method (Oda and Iwashita 2000). In parts where the normalized micro-curvatures (κ_2^*) are nearly zero, the material behaves as a rigid body. The sign of normalized micro-curvature (κ_2^*) is sharply switched at the middle of shear band, shown in Figure 2.

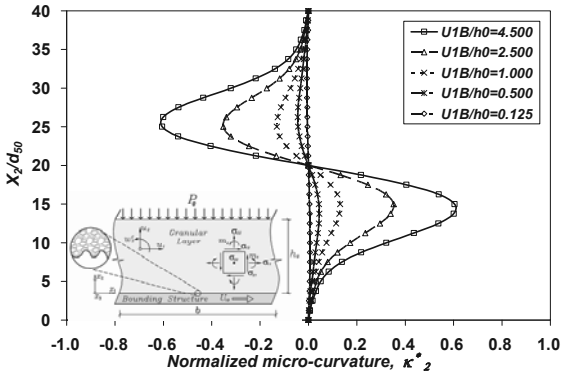

Figure 2. Distribution of normalized micro-curvature across normalized height of granular layer under $P_0 = 100\ kPa$ for different U_{1B}/h_0 ($e_0 = 0.6$, $d_{50} = 1\ mm$).

Figure 3 illustrates the non-uniform distribution of normalized couple stresses (m_2^*) across the normalized height of granular layer. As displayed in this figure, the distribution of m_2^* is critically non-linear where the horizontal displacement of bounding structure increases. The variation of m_2^* depends significantly on the values of horizontal displacement applied to the bounding structure. Although, couple stress within the shear band cannot be measured experimentally due to its small magnitude, it can be detected by soil grain rotation which is visible in the experiments (Hall et al. 2010) and DEM simulations (Oda and Iwashita 2000).

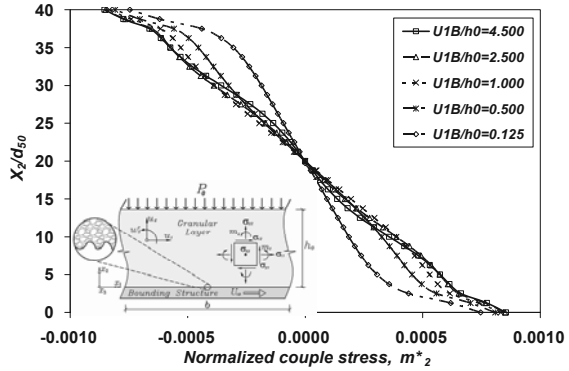

Figure 3. Distribution of normalized couple stress across normalized height of granular layer under $P_0 = 100\ kPa$ for different U_{1B}/h_0 ($e_0 = 0.6$, $d_{50} = 1\ mm$).

According to the Figures 1-3, micro-polar quantities are noticeable within the shear band during plane shearing. The shear band is characterized by significant Cosserat rotations and pronounced micro-curvatures. High quantities of couple stresses are obtained at the shear band edges. The contour plot of void ratio and deformed configuration of granular layer in the residual state for an initially homogeneous void ratio of $e_0 = 0.6$ after horizontal displacement of $u_{1B} = 1.50\ h_0$ are presented in Figure 4. The brighter zones, in the plot, are of higher void ratios as a result of dilatancy or where failure may start. Based on this figure, the deformation of large shearing are obviously concentrated within a narrow band at the middle of the layer. The predicted thickness of shear band is about 23 d_{50}.

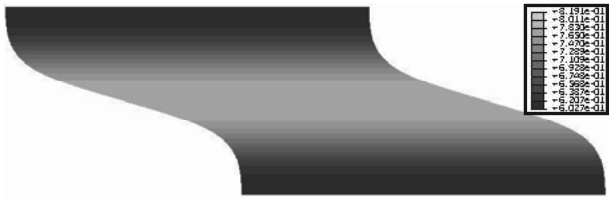

Figure 4. Deformed configuration of granular layer under $P_0 = 100\ kPa$ after $U_{1B} = 1.5\ h_0$ along with contour plot of void ratio ($e_0 = 0.6$, $d_{50} = 1\ mm$)

Herein, the shear band formation is investigated in a biaxial compression test. For numerical modeling, a dry granular cuboid with a height $h_0 = 20\ cm$, a width $b = 8\ cm$ and a unit depth is considered. The specimen is laterally confined by an external pressure of 70 kPa and kept between two opposing horizontal plates. In finite element calculations, initial homogeneous state is assumed with initial void ratio, ($e_0 = 0.6$) and mean grain diameter, ($d_{50} = 1\ mm$). Afterwards, the axial quasi-static deformation in granular material is initiated through a constant vertical displacement increment prescribed to the top plate. Finite element simulations of biaxial compression test are carried out for three different element sizes. The finite element meshes consist of 640, 2560 and 10240 elements. The deformed meshes along with contour plots of void ratio at vertical compression of $u_2/h_0 = 10\%$ are presented in Figure 5. The complete shear band is already emerged shortly after the peak state. This result coincides with the solution of a bifurcation analysis (Vardoulakis 1980). Shear band is characterized by an increase of void ratio (Figure 5). This result confirms the experimental findings by Desrues et al. (1996). The width of shear band has an almost constant value of 14 d_{50} for all mesh sizes. The inclination of shear band with respect to the horizontal axis has a nearly constant value of 55˚. Both the thickness and inclination of shear band are in satisfying agreement with the experimental results (Alshibli and Sture 2000).

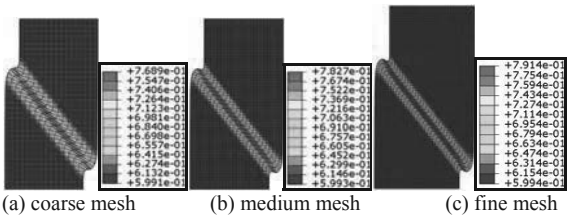

(a) coarse mesh (b) medium mesh (c) fine mesh

Figure 5. Deformed finite element mesh along with contour plot of void ratio for (a) coarse mesh, (b) medium mesh, and (c) fine mesh

It has been reported from experimental observations of biaxial compression tests (Alshibli and Sture 2000) that the behavior of granular materials is dependent on the boundary conditions of specimen. The following simulations illustrate the boundary condition effect on the shear band formation. The finite element calculations are performed for two separate cases: (1) smooth and (2) very rough surfaces at the top and bottom of specimen. The obtained finite element results are compared with those of experiments (Alshibli and Sture 2000). Figure 6 displays that multiple shear bands develop in the specimen when the bottom boundary is very rough (Figures 6(c) and 6(d)). The finite element results demonstrate that shear band location and mode are highly influenced by the prescribed boundary conditions, prescribed along the top and bottom surfaces of specimen (Figures 6(a) and 6(c)), which are consistent with experimental observations (Figures 6(b) and 6(d)) (Alshibli and Sture 2000). According to finite element results, two principal mechanisms of shear banding may occur in granular materials under plane strain compression: in the first mechanism, a single shear band is formed inside the specimen (Figures 6(a) and 6(b)), while in the second, more than one shear band can occur if the movement of bottom boundary is restrained under plane strain condition (Figures 6(c) and 6(d)).

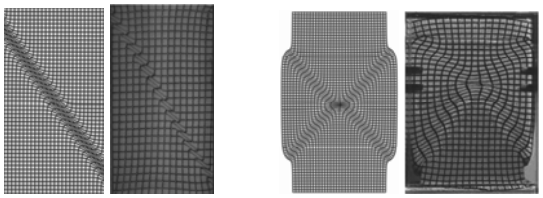

(a) (b) (c) (d)

Figure 6. Comparison between shear banding patterns obtained from numerical simulations and experiments (Alshibli and Sture 2000): (a) and (b) free rotational boundary, (c) and (d) restrained rotational boundary

The behavior of granular material is also affected by the geometry of specimen. If the length to width ratio of specimen would be larger than 2.0, then the failure will not, to some extent, be affected by the boundary conditions and a single shear band is formed (Figure 5). For the ratio equal to 2.0, a complicated pattern of shear banding is developed within the specimen, as shown in Figures 7(a)-7(c). For smaller values of length to width ratio, a reflection of shear band is observed when it hits the bottom rigid boundary (Figures 7(d)-7(f)).

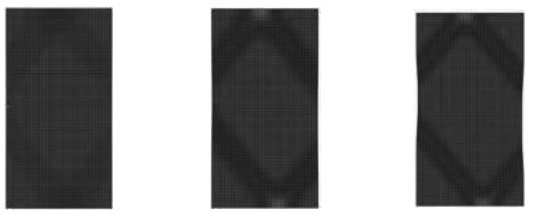

Axial strain = 2% Axial strain = 5% Axial strain = 13%
(a) (b) (c)

Axial strain = 0% Axial strain = 5% Axial strain = 13%
(d) (e) (f)

Figure 7. Shear band formation process in biaxial specimen with different geometries: (a), (b), (c) length to width ratio = 2, and (d), (e), (f) length to width ratio = 1.33

5 CONCLUSION

An extended elasto-plastic Lade's model along with embedded Cosserat rotations and couple stresses, can simulate properly the localization phenomenon in the granular materials under different loading conditions. Polar quantities are noticeable in the shear band. Cosserat rotations, increasing void ratios, high gradient of micro-curvatures and couple stresses can be used to identify the shear band. The couple stress values is found to be very small in magnitude compared with the stresses; however, they have significant effects on the material behavior, partucularly in the softening regime. Location and evolution of shear bands are mainly affected by the micro-polar kinematical boundary conditions and rotation resistance of soil grains prescribed along the boundries. The length scale and size of specimens have substantial influence on observed pattern of shear banding in granular materials.

6 REFERENCES

Hall S.A., Bornert M., Desrues J., Pannier Y., Lenoir N., Viggiani G. and Bésuelle P. 2010. Discrete and continuum analysis of localised deformation in sand using X-ray μCT and volumetric digital image correlation. *Géotechnique* 60(5), 315-322.

de Borst R. 1991. Simulation of strain localization: a reappraisal of the Cosserat continuum. *Engineering Computations* 8, 317–332.

Mühlhaus H.B. 1986. Shear band analysis in granular materials by Cosserat theory. *Ingenieur Archiv* 56, 389-399.

Vardoulakis I. and Sulem J. 1995. *Bifurcation Analysis in Geomechanics*. Blackie Academic & Professional, Glasgow, UK.

Lade P.V. and Kim M.K. 1988. Single hardening plasticity model for frictional materials. *Computers and Geotechnics* 6, 13-29.

Kim M.K. and Lade P.V. 1988. Single hardening constitutive model for frictional materials. *Computers and Geotechnics* 5, 307-324.

Ebrahimian B., Noorzad A. and Alsaleh M.I. 2012. Modeling shear localization along granular soil–structure interfaces using elasto-plastic Cosserat continuum. *International Journal of Solids and Structures* 49, 257–278.

Oda M. and Iwashita K. 2000. Study on couple stresses and shear band development in granular media based on numerical simulation analyses. *International Journal of Engineering Science* 38, 1713-1740.

Vardoulakis I. 1980. Shear band inclination and shear modulus in biaxial tests. *International Journal of Numerical and Analytical Methods in Geomechanics* 4, 103-119.

Desrues J., Chambon R., Mokni M. and Mazerolle F. 1996. Void ratio evolution inside shear bands in triaxial sand specimens studied by computed tomography. *Géotechnique* 46, 529-546.

Alshibli K.A. and Sture S. 2000. Shear band formation in plane strain experiments of sand. *ASCE Journal of geotechnical and geoenvironmental engineering* 126(6), 495-503.